International Journal of Thermal Sciences 48 (2009) 1707–1717

Contents lists available at ScienceDirect

International Journal of Thermal Sciences

journal homepage: www.elsevier.com/locate/ijts

Thermal shielding of multilayer walls with phase change materials under different transient boundary conditions

François Mathieu-Potvin, Louis Gosselin*

Département de génie mécanique, Université Laval, 1065 avenue de la Medecine, Québec City, Québec, Canada G1V 0A6

ARTICLE INFO

Article history:
Received 24 September 2008
Received in revised form
27 January 2009
Accepted 28 January 2009
Available online 19 March 2009

Keywords:
Multilayer wall
Phase change material (PCM)
Heat gain
Heat loss
Genetic algorithms
Building envelope

ABSTRACT

A numerical model is presented to determine the thermal shielding performance of an exterior wall (e.g., building envelope) containing layers of PCMs. The model is exploited to perform a parametric study to assess the influence of the position and melting temperature of one PCM layer. Results showed that benefits are to be expected when the interior and exterior temperatures are close. Then, the wall composition has been optimized with a genetic algorithm based on a yearly analysis with the possibility of including several PCM layers. Idealized weather conditions and measured weather conditions (including solar radiation) have been considered. Results showed that for Québec City, optimal south-facing wall includes one PCM layer when real weather data are considered. Its effect is to shield the heat transfer in the summer. This paper provides a fundamental understanding of multilayer walls with PCMs.

1. Introduction

Building walls are designed to provide high thermal resistance (i.e., R-factor), and thus include low thermal conductivity materials (insulators). In a thermal steady-state regime, a low thermal conductivity wall results in low heat gains and heat losses which are beneficial to reduce energy consumption. However, the thermal regime is never steady in practice, but rather in a quasi-periodic regime due to the day/night and winter/summer alternations. These thermal cycles induce an oscillatory heat loss/gain which is detrimental to the HVAC energy consumption and to thermal comfort. Therefore, in addition to providing a high R-factor, walls should possess a good thermal inertia (i.e., volumetric heat capacity) to attenuate and delay exterior fluctuations, thus protecting the indoor thermal state. However, insulator materials typically have a very limited energy storage potential, and vice versa. When it comes to selecting the wall composition, there is thus a competition between two opposing requirements: low thermal conductivity and large thermal inertia. By combining both types of materials, one could benefit from their respective advantages and limit their drawbacks.

The optimal thickness of a composite wall is investigated in Ref. [1], taking into account different energy cost. Asan studied different arrangements of insulator and thermal mass within the wall and found that a situation where insulation is divided in two (half of it close to the inner surface and the other close to the outer surface) gives the highest time lags and the largest decrement factors [2]. Later, he reported the time lags and decrement factors for different building materials based on a numerical investigation [3]. The optimal sequence of resistive and capacitive layers within building envelope is determined by Ciampi et al. [4], in order to minimize the air-conditioning plant intervention to keep the indoor air temperature constant against sinusoidal and impulsive external temperature variations. These studies showed the potential of combining different types of materials (i.e., insulator and thermal mass) to improve the thermal performance of the wall.

With their huge heat storage capacity per unit of volume, phase change materials (PCMs) have received a lot of attention lately to work as passive building thermal regulators [5]. A PCM layer in a wall will melt at a constant temperature when the exterior temperature rises, and solidify when the exterior temperature goes down, in such a way that the indoor could become relatively blind to the exterior conditions. In Ref. [6], a numerical analysis is performed for composite plates made of several PCMs, which are used as energy storage components. The authors noted an improvement with multiple PCM plates compared to the one PCM plates. Alawashi [7] performed a thermal analysis of a wall containing cylindrical PCM intrusions, and observed a reduction in heat flow through the wall during working hours. Ismail and Castro [8]

* Corresponding author. Tel.: +1 418 656 7829; fax: +1 418 656 7415.
E-mail address: Louis.Gosselin@gmc.ulaval.ca (L. Gosselin).

1290-0729/$ – see front matter © 2009 Elsevier Masson SAS. All rights reserved.
doi:10.1016/j.ijthermalsci.2009.01.010

Nomenclature

c_p	heat capacity, J/kg K
f_l	liquid fraction
G_{sun}	solar irradiation, W/m^2
h	heat transfer coefficient, W/m^2 K
k	thermal conductivity, W/m K
L	wall thickness, m
N_{gen}	number of generations for convergence
q''	heat flux, W/m^2
q''_L	PCM l.h.s. heat flux, W/m^2
q''_R	PCM r.h.s. heat flux, W/m^2
q	heat flow in a period, J/m^2
$\tilde{q}$	relative heat flow
S	slab position, m
T	temperature, °C
$\overline{T}$	average temperature, °C
ΔT	temperature amplitude, °C
t	time, s
x	coordinate in the wall, m
x_{eq}	equilibrium PCM position, m

Greek symbols

α	solar absorptivity
ρ	density, kg/m^3
λ	latent heat, J/kg
ω	angular frequency, 1/s

Subscripts

day	relative to a daily period
ext	exterior
int	interior
l	liquidus
m	melting
opt	optimal
PCM	phase change material
ref	with insulator only (reference)
s	solidus
year	relative to an annual period

studied a room in real operating condition with PCM filled walls. Results showed that using PCM slab in walls reduced the HVAC energy consumption of 20–30% compared to a conventional wall. Kim and Darkwa [9] compared the thermal performance of a laminated-PCM wall and a dispersed-PCM wall. It was found that the laminated-PCM wall is the configuration that yields the best thermal performance. Kuznik [10] performed experimental and numerical analysis of a room with walls containing a PCM slab. The authors noted lower indoor temperature fluctuations compared to wall without PCM slabs. Helmut and Stetiu [11] simulated a standard room with PCM wallboard under Californian climate conditions. They found that, for a warm seven-day period, PCM wallboards carried better thermal comfort. Heim and Clarke [12] treated numerically a three-room system with PCM slabs at the wall indoor sides, and sensible room temperature reduction was noticed.

Most of the above-mentioned papers on PCMs consider nearly tropical climates, i.e., when the inside temperature is typically within the daily temperature range. Cold climates or seasons are often disregarded. Also, the fundamental thermal behavior of multilayer walls with PCMs has not been investigated, contrarily to that of multilayer walls without PCM which have received a lot of attention lately, e.g., Refs. [1–4]. Furthermore, the formal optimization of the design of walls with PCM is yet to be addressed. In this paper, we first investigate the thermal response of a multilayer wall with PCMs under idealized (sinusoidal) boundary conditions. The model is voluntary fundamental (1-D heat transfer, periodic regime) so that results provide an insight on how walls with PCMs behave, and thus help to understand further analysis where PCM-walls are integrated in real and more complex building envelopes, with various architectures, locations and weathers. Thanks to the fundamental approach retained here, results could be extended to non-building walls with PCM (e.g., heat storage and recuperators). Nevertheless, temperature ranges and material properties that are common in buildings are used here. The objectives of this paper are: i) to understand how the thermal performance of a multilayer wall is influenced by the presence of PCMs, ii) to develop an optimization method in order to design walls with PCMs, and iii) to determine the potential benefit of such a wall with more realistic boundary conditions (especially for colder climates). To achieve objective (i), a parametric study of the effect of a PCM layer position and melting temperature is presented. For objective (ii), the optimization of the material composition of the wall is performed with a genetic algorithm (GA) that chooses a material for each wall layer among a database of materials that includes many PCMs. The GA minimizes the absolute heat flux at the interior surface of the wall. Finally, for objective (iii), a parametric study and a GA optimization are also performed, but with real weather data (outside temperature and irradiation impinging the wall) from Québec City (QC, Canada), rather than with idealized boundary conditions.

2. Problem formulation

Consider a 1D multilayer wall such as that shown in Fig. 1. The wall has a thickness L and is separated into several layers, including some that can be made of PCMs. The energy equation in the wall reads as

$$\rho c_p \frac{\partial T}{\partial t} = \frac{\partial}{\partial x}\left(k\frac{\partial T}{\partial x}\right) - \rho\lambda\frac{\partial f_l}{\partial t} \tag{1}$$

The last term takes into account the latent energy associated with phase changes when they occur. The latent heat is λ, and it is a function of x in our problem. When a layer is not a PCM, its associated λ-value is zero. The liquid fraction f_l at a given position is the percentage of the latent heat that has been absorbed at a given time, and is calculated here by

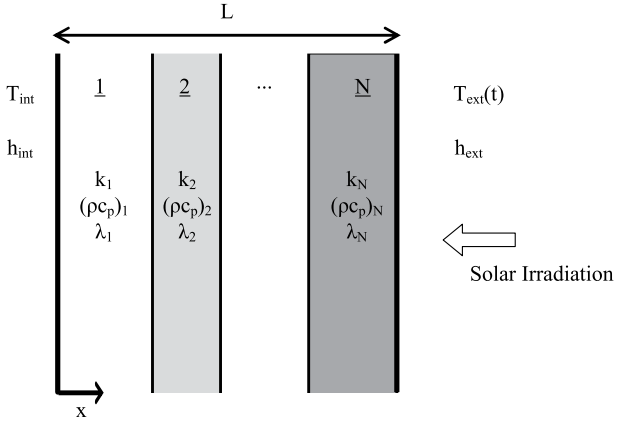

Fig. 1. Schematic representation of a 1D multilayer wall.

$$f_l = \begin{cases} 1 & T \geq T_l \\ \dfrac{T - T_s}{T_l - T_s} & T_s \leq T \leq T_l \\ 0 & T \leq T_s \end{cases} \quad (2)$$

Natural convection in the PCM is neglected in this work (i.e., encapsulated PCMs). Solving Eq. (1) requires boundary conditions. We first suppose that the exterior temperature varies cyclically and assumes a sinusoidal pattern of angular frequency ω ($\omega = 2\pi/(24\text{ h} \times 3600\text{ s})$),

$$T_{ext}(t) = \overline{T}_{ext} + \Delta T_{ext}\cos(\omega t) \quad (3)$$

This assumption will be relaxed later in the paper with real weather data and solar irradiation. In all cases tested with the idealized outdoor temperature of Eq. (3), the value of ΔT_{ext} was set to 5 °C based on typical climatic data reported in Refs. [13,14].

The indoor temperature is assumed constant and was set to $T_{int} = 22$ °C. In other words we assumed that the interior temperature is always maintained at that temperature by the HVAC system, in line with work on multilayer walls, for example in Refs. [2,3]. To understand the consequence of this choice of boundary condition, recall that PCMs (and other large thermal inertia materials) in real building walls have two purposes: (i) damp the indoor air temperature variations thanks to their thermal inertia, and (ii) shield the exterior weather variation by cyclically absorbing and releasing thermal energy from and to the outdoor air. The damping ability of the wall would be demonstrated if T_{int} was variable, but this time-dependant behavior would depend on the interactions with other hypothetical building components, which would be case-specific. On the other hand, by setting T_{int} as constant, only the shielding ability of the wall is revealed, i.e., its capacity to attenuate heat flux variations that reach the indoor air at $x = 0$. Thus, for generality reasons, the indoor temperature is assumed to be maintained constant in time, and the results presented in this article focus on the shielding performance of the wall.

Convection boundary conditions are applied on each side of the wall:

$$\begin{aligned} -k\left.\frac{\partial T}{\partial x}\right|_{x=0} &= h_{int}(T_{int} - T(x=0)) \\ -k\left.\frac{\partial T}{\partial x}\right|_{x=L} &= h_{ext}(T(x=L) - T_{ext}) \end{aligned} \quad (4)$$

The convection coefficients used in this study were $h_{int} = 10$ W/m^2 K and $h_{ext} = 35$ W/m^2 K based on typical values reported in Ref. [15] and they include radiation exchanged with surroundings. In practice, the convection coefficient (in particular h_{ext}) will vary with time according to airflow conditions. However, since the convection thermal resistance is small compared to that of the wall, assuming $h \approx$ constant should not affect significantly the results. The aforementioned boundary conditions emphasize the link between the fundamental model of the wall used here and an eventual integration in building design. Solar irradiation will be included explicitly later in the text with real weather data.

When solving Eqs. (1)–(4) (idealized boundary conditions), we seek for the periodic solution, i.e., when the temperature and liquid fraction profiles repeat exactly every cycle. In other words, we will not be interested in the initial transient regime when considering idealized boundary conditions.

The figure of merit that we investigate in this paper is the energy flow through the interior surface ($x = 0$) for a period of interest. When this heat flow is positive, energy is added to the building and cooling must be provided by the HVAC system. On the other hand, when the heat flow is negative, heat is removed from the building and the HVAC system must compensate the loss. Because a detrimental energy effect is observed whether the heat flow is positive or negative, the function that we will minimize is written as follows:

$$q = \int \left| -k\frac{\partial T}{\partial x}(x=0) \right| dt \quad \text{(to minimize)} \quad (5)$$

The period over which the integral of Eq. (5) is performed depends on the outdoor temperature form. For the harmonic boundary condition of Eq. (3), this period is one day; q becomes q_{day}. Later in the text, thermal analysis of the wall is performed for an entire year with more realistic weather data. Then the integral in Eq. (5) is performed over a full year; q becomes q_{year}.

The minimization of q will be achieved by varying the wall composition (see Sections 5 and 9). In particular, three types of materials are considered: insulation, concrete and PCM. Their thermal properties are listed in Table 1. Concrete is often considered to add thermal inertia in a building system. The properties of the PCM are that of typical paraffins. Paraffins have been considered here because they are among the most suitable to construction, they are stable and their cost is moderate [5]. Looking at Table 1, we observe that the thermal conductivity of the PCM is larger than that of the insulator. In other words, even though PCMs provide a large thermal inertia, they tend to conduct heat somewhat more easily than insulators. Therefore, we expect that the optimal tradeoff wall will offer a balance of PCMs and insulators. An additional property of PCMs is their melting temperature. Many types of paraffins are available on the market, each having thermal properties similar to that shown in Table 1, but with different melting temperatures T_m. Therefore, melting temperatures for this type of PCM can be considered as a design variable. PCMs with various melting temperatures will be considered later in this paper, with the other thermal properties as shown in Table 1.

3. Numerical model

A finite-volume code has been developed in order to determine the temperature in a multilayer wall with PCMs. The boundary condition can be idealized (Eq. (3)) or based on real weather data. The wall was discretized in small control volumes, and Eq. (1) was integrated on each control volume. After interpolations, the resulting set of algebraic equations was solved iteratively in MATLAB. An iterative procedure is required because of the non-linearity introduced by the phase change (i.e., the last term of Eq. (1)). Convergence at a given time step is declared when the maximal local difference between the temperature at the actual iteration and that of the preceding iteration is smaller than 10^{-5} °C. A similar criterion was used for f_l as well. The solver was confronted to the analytical solution of the Stefan problem which consists in determining the evolution of the solid–liquid interface in a semi-infinite slab [17]. Our code yielded the same interface position in time as that of the analytical solution. In all of our calculation, we assumed that T_l and T_s were equal to $T_m + 0.5$ °C and $T_m - 0.5$ °C respectively.

To find the periodic regime (i.e., when Eq. (3) is applied on the outside boundary of the wall), our solver advances in time and calculates the temperature in the next cycle until the maximal local temperature difference between two consecutive cycles is less than 10^{-2} °C. A similar criterion is also used for f_l before declaring that

Table 1
Thermal properties of the materials considered [16].

Material	k (W/m K)	ρc_p (J/m^3 K)	λ (J/kg)
Insulator (polystyrene)	0.027	66,550	0
Concrete	0.720	1,450,800	0
PCM (common paraffins)	0.200	1,600,000	200,000

periodicity is achieved. Mesh and time-step independence will be described later in the text.

4. Parametric study of the influence of a PCM layer

Before performing full optimizations of a wall structure for given sets of weather data, it is instructive to study the effect of a PCM layer within the wall under idealized harmonic boundary conditions. Understanding how a PCM layer influences the overall wall thermal behavior will help to analyze the optimization results presented in subsequent sections. The two main parameters that we analyze in this section are: i) the position of the PCM layer within the wall, and ii) the melting temperature of the PCM. In particular, we want to assess the effect of these design parameters for different outdoor conditions.

4.1. Qualitative analysis of an ideal wall with one PCM layer

Suppose a wall made of a hypothetical material with high thermal resistance and negligible heat capacity (insulator). A constant temperature T_{int} is imposed on its left side, and a harmonic (periodic) temperature T_{ext} is imposed on its right side, Fig. 2a. Note that T_{int} is in the range of T_{ext}, see Fig. 2a. The value of interest, i.e., the heat flux at $x = 0$ is sketched in the r.h.s. of Fig. 2b. Recall that our goal is to diminish the absolute area under this curve, see Eq. (5). We want to describe in this section how an ideal PCM layer (infinitely thin, melting at constant temperature T_m, infinite conductivity, and large latent heat) would influence the heat flux at $x = 0$.

For this purpose, consider an ideal PCM layer at a position where the total energy flow entering the PCM from the left (q''_L) is equal to the total (harmonic) energy flow leaving the PCM from the right (q''_R) integrated over a cycle, see Fig. 2c. Geometrically, this means that the PCM is inserted at the position where the average temperature profile without PCM (dashed line, Fig. 2c) is equal to T_m. In other words, the average T profile is not affected by the PCM in that particular case. The equilibrium position is $x_{eq}/L = (T_{int} - T_m)/(T_{int} - T_{ext})$. An energy balance on the PCM yields:

$$k\frac{T_{int} - T_m}{x_{eq}} - k\frac{T_m - \overline{T}_{ext}}{L - x_{eq}} + k\frac{\Delta T\cos(\omega t)}{L - x_{eq}} = \rho\lambda \times \text{thickness} \times \frac{df_l}{dt} \tag{6}$$

which means that $f_l \sim \sin(\omega t)$, and that for f_l to be bounded between 0 and 1, the minimal thickness of PCM is

$$\text{thickness} = \frac{2k\Delta T(T_{int} - \overline{T}_{ext})}{\rho\lambda L\omega(T_m - \overline{T}_{ext})} \tag{7}$$

The heat flux at $x = 0$ resulting from this configuration is a constant, see r.h.s. of Fig. 2c. The result is that the area (Eq. (5)) under this curve is smaller than that of the wall with no PCM from Fig. 2b. Hence, this illustrates how a PCM layer may diminish the total energy flow at $x = 0$. Note that for the special case $T_{int} = T_m = \overline{T}_{ext}$, all PCM-positions in the wall provide an effect as that described in this paragraph, thus the PCM layer provides perfect shielding since the temperature slope is nil at $x = 0$.

Now, let us explain what happens when one moves this PCM from that equilibrium position. For this purpose, we first displace the PCM layer toward the left side, see Fig. 2d. The first two left handside term of Eq. (6) will not be zero if $x \neq x_{eq}$. They will assume positive value. Integrating Eq. (6) over time will result, in addition to the harmonic component, in a constantly increasing term. In other words, the slab will eventually melt completely and the periodic regime includes a time span over which the PCM shielding

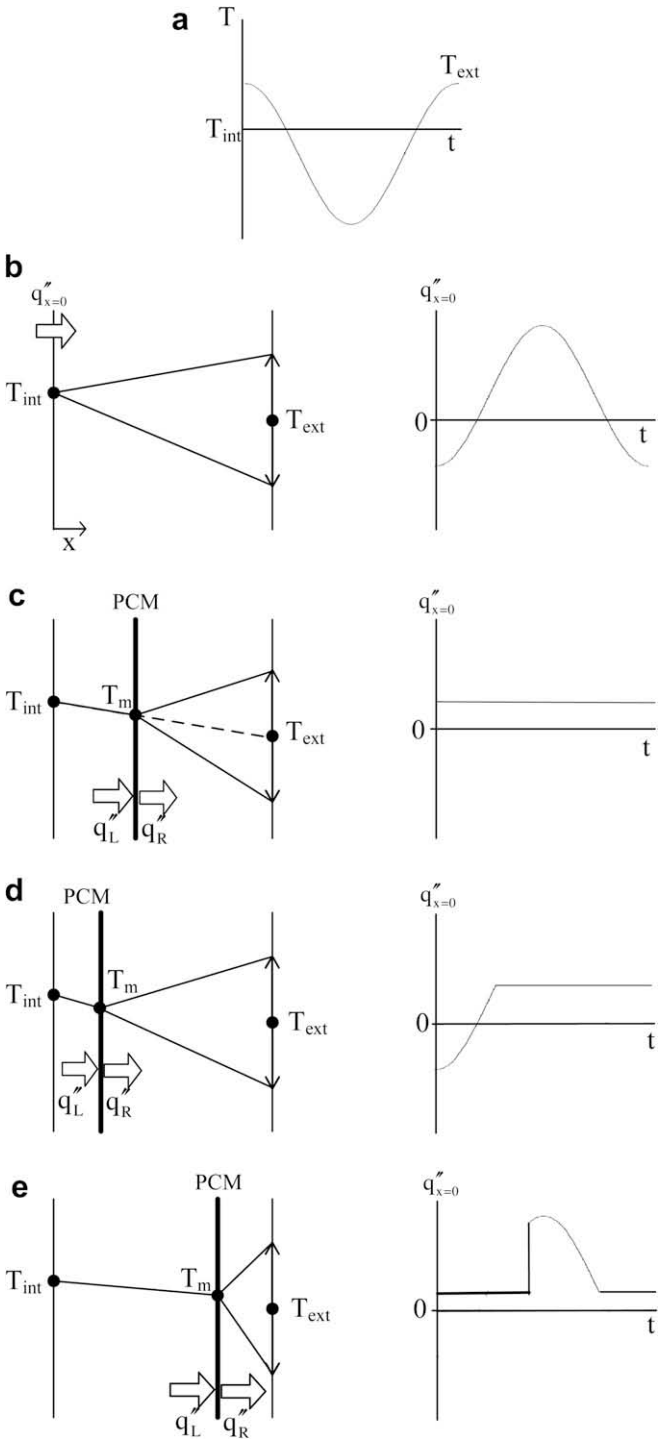

Fig. 2. Temperature profile of an idealized wall while the PCM layer is melting (T_{int} is in the range of $\overline{T}_{ext}$).

effect is not present, even with a very large λ-value. During the period when the PCM is active, the temperature profile near the left wall is steeper than in Fig. 2c; hence the constant part of the heat flux is larger, which is detrimental compared to the equilibrium position. On the other hand, for the rest of the cycle, the PCM is completely melted and the heat flux undertakes a harmonic behavior crossing the zero heat flux value at a certain time, which can be beneficial depending on the amplitude of this harmonic behavior, see Fig. 2d. Overall, a PCM position toward the interior

side of the wall may yields the right tradeoff between these two competitive phenomena and provides a minimum total energy flow.

The opposite phenomena happen when we displace the PCM layer toward the right side (i.e., exterior) of our hypothetical wall, see Fig. 2e. During a certain time span, the slab is completely solid. During melting, the constant value of the heat flux at $x=0$ is smaller since the temperature slope on the left side of the wall is less steep; this is favorable, see r.h.s. of Fig. 2e. On the other hand, for the rest of the cycle, the PCM is completely solidified and the heat flux at $x=0$ undertakes a harmonic behavior, with large and positive value; this is detrimental. To summarize, we illustrated that when T_{int} is in the range of T_{ext}, a PCM layer may yield smaller overall energy flow and that an optimal position for this PCM layer may exist on either side of the wall.

Now we wonder how the optimal melting temperature and the optimal position are related. When we fix the position of the PCM, we see that as T_m approaches T_{int}, during the phase change of the PCM, the slope of the temperature at $x=0$ diminishes, which leads to a small constant energy flow in Fig. 2c–e. We conclude that the optimal T_m-value should be near the T_{int} value.

Now, let us explain what happens when the melting temperature is not between T_{int} and $\overline{T}_{ext}$. For example, suppose that we want to place a PCM with $T_m > T_{int}$ in Fig. 2b. The melting temperature T_m will have to be in the temperature 'cone' (drawn in Fig. 2b) in order to experience phase change. Thus, as T_m differs from the interval $[T_{int}, \overline{T}_{ext}]$, the PCM slab will have to move toward the exterior side of the wall. To summarize, we expect that for these cases, i.e., $T_m \notin [T_{int}, \overline{T}_{ext}]$, the optimal PCM position should be closer to the r.h.s of the wall.

To close this qualitative analysis of how a PCM slab influences the thermal behavior of a wall, we investigate the case when the temperature on the left side T_{int} is not in the range of the temperature on the right side (T_{ext}), see Fig. 3a. When the wall has no PCM layer (Fig. 3b), the heat flux at $x=0$ is obviously harmonic. Now, consider a PCM layer positioned at the equilibrium, i.e., where the energy flow entering the PCM on the left side q''_L equals the total energy flow leaving the PCM on the right side q''_R when integrating in time. In this arrangement, the PCM is always at its melting temperature T_m. The heat flux at $x=0$ resulting from this configuration is constant, see r.h.s. of Fig. 3c, but more importantly, the area under this curve is exactly the same as that of the wall without PCM from Fig. 3b. This is because the heat flux curve in Fig. 3b is all on the same side of the abscises, hence, flattening this curve does not change the integral value, contrarily to the case shown in Fig. 2. From this qualitative analysis, we expect that there is no optimization opportunity in this case, i.e., when $T_{int} \notin T_{ext}$.

In conclusion, the main results for a wall subject to a harmonic exterior temperature with only one PCM layer could be summarized as

(i) For $T_{int} \in T_{ext}$, there is an optimal position and melting temperature for the PCM layer;
(ii) For $T_m \notin [T_{int}, \overline{T}_{ext}]$, the optimal position is toward the exterior side of the wall;
(iii) The optimal T_m is near T_{int};
(iv) For $T_{int} \approx T_m \approx \overline{T}_{ext}$, the total heat flow is insensitive to the PCM position;
(v) For $T_{int} \notin T_{ext}$, there are no optimization opportunities using a PCM layer.

These four conclusions were obtained by qualitative arguments, and they should be verified numerically. This is what we present in the next paragraphs.

4.2. Numerical analysis of a wall with one PCM layer

Now that we have gained a better understanding of the impact of PCMs in walls (Section 4.1), we investigate walls with non-idealized thermophysical properties. For the sake of illustration, we considered a 10 cm-thick wall as shown in Fig. 4. The wall is made of insulator, with one layer of PCM with a thickness of 0.5 cm. For

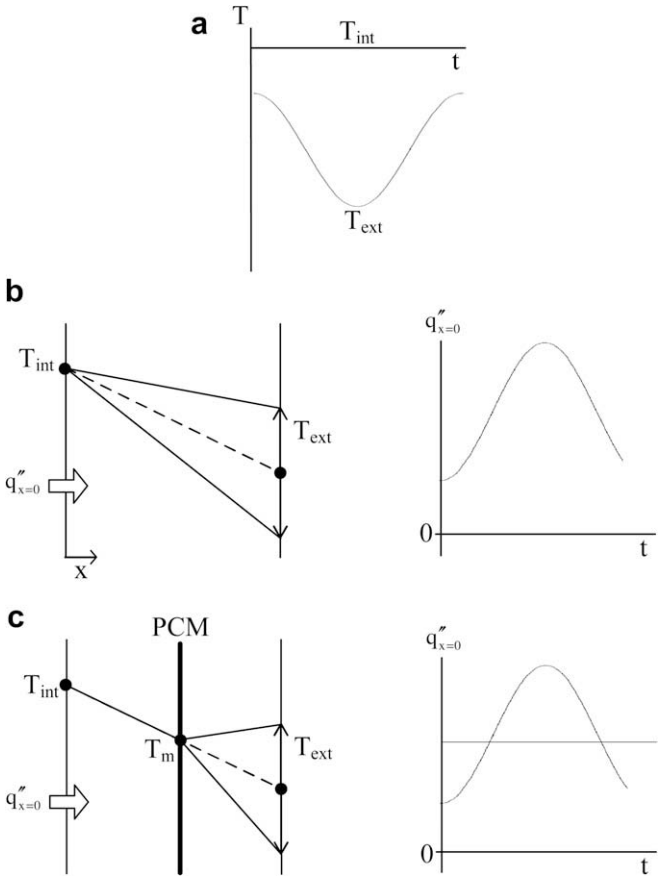

Fig. 3. Temperature profile of an idealized wall while the PCM layer is melting (T_{int} is not in the range of $\overline{T}_{ext}$).

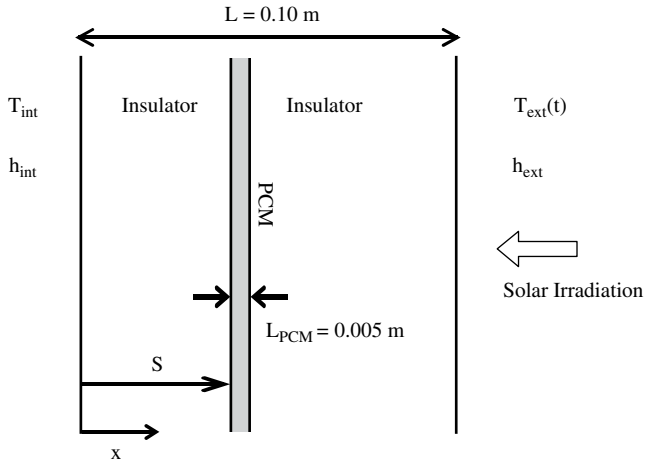

Fig. 4. Wall configuration for parametric study.

different idealized weather conditions (i.e., outdoor temperature following Eq. (3)), the melting temperature T_m of the PCM layer and its position S within the wall will be varied in order to observe which design leads to the best performance. The period considered is 1 day (i.e., $\omega = 2\pi/24$). The results reported are for the periodic regime. The daily absolute heat transfer q_{day}, Eq. (5), has been normalized with a reference in order to facilitate the analysis

$$\tilde{q}_{day} = \frac{q_{day}}{q_{day,ref}} \tag{8}$$

$q_{day,ref}$ corresponds to the daily absolute heat transfer with a wall containing only an insulator (i.e., no PCM). When $\tilde{q}_{day}$ is lower than 1, then the PCM is useful. Otherwise, when $\tilde{q}_{day}$ is greater than 1, the PCM is detrimental to the wall thermal performance.

Mesh and time-step independence were tested extensively. Mesh was refined by successive doubling up to the point when the heat flow q (satisfying time-step independence) varied by less than 0.5%. The time-step independence for each mesh is satisfied when the heat flow q varies by less than 0.1% for two consecutive time-step division by 2. The results showed that for the conditions considered, 130 control volumes with a time step of 43.2 s (1/2000 day) were sufficient to provide that precision. This numerical setup will be used in Sections 4 and 6.

4.2.1. Case I: $T_{int} = \overline{T}_{ext}$

First let us consider the case when $T_{int} = \overline{T}_{ext}$. Fig. 5 shows the values of $\tilde{q}_{day}$ achieved with the wall of Fig. 4 for different positions and melting temperatures of the PCM. Most of the times, $\tilde{q}_{day}$ is smaller than 1 which indicated that the PCM is beneficial. Furthermore, the melting temperature has a strong effect on the performance. We observe that a melting temperature of 22 °C (i.e., the average temperature within the wall) is optimal, which corresponds to results stated in the end of Section 4.1 (i.e., $T_{m,opt}$ near T_{int}). The optimal layer position is in the middle of the wall which is indicated by a small black circle in Fig. 5. In that case, the absolute heat transfer dropped by 98% compared with the reference wall with insulator only and the heat flux at $x = 0$ is almost zero throughout the day. For this special thermal configuration, i.e., $T_m = T_{int} = T_{ext} = 22$ °C, the curve is almost insensitive to PCM layer position, as predicted in Section 4.1. We can also observe that the optimal position S increases (i.e., moves toward the exterior side of the wall) as T_m differs from T_{int}. This trend was expected from the qualitative analysis. The exceptions are for large (or small) T_m-value curves, for which the heat capacity of the wall (phase lag) dominates the phase change (shielding) phenomena. In these cases, our simulations yielded optimal position S at the center of the wall, which corroborates with other works [2]. From the symmetry of the boundary conditions, the curves with $T_m = 21$, 20, 19, 18, 17 °C are the same as those with $T_m = 23$, 24, 25, 26, 27 °C, respectively. It was verified numerically but it is not shown in Fig. 5 for clarity.

The exterior daily average temperature will vary in time, and it is important to verify whether the performance of the design achieved with a given $\overline{T}_{ext}$ is sensible to exterior variations. In other words, we need to assess the robustness of the optimal design found when $\overline{T}_{ext} = 22$ °C (i.e., $S = 0.0475$ m and $T_m = 22$ °C) for other weather conditions. Keeping that design, we varied $\overline{T}_{ext}$ and calculated $\tilde{q}_{day}$ in each case. Results are reported in Fig. 6. As the outdoor temperature differs from the indoor temperature (22 °C), the shielding performance of the wall decreases. For outdoor temperature smaller than ~18 °C or larger than ~26 °C, the designed wall performance is worst than a wall made of insulator only. The symmetry of Fig. 6 is obvious since $T_{int} = T_m$.

4.2.2. Case II: $T_{int} \neq \overline{T}_{ext}$, but T_{int} within the range of $T_{ext}(t)$

In this subsection we consider the case when T_{int} is within the range of $T_{ext}(t)$ but not necessarily equal to $\overline{T}_{ext}$. The melting temperature of the PCM slab and its position in the wall has been varied, and the daily absolute heat transfer calculated for the case where $\overline{T}_{ext} = 20$ °C, i.e., 2 °C less than the indoor temperature. Results are provided in Fig. 7. The minimal $\tilde{q}_{day}$ value is still reached when $T_m = 22$ °C. This corresponds to the value expected from the qualitative analysis from Section 4.1, i.e., $T_{m,opt}$ near T_{int}. The position has little effect on the daily heat flow for this melting temperature, but the optimal position of the PCM is found at $S = 0.006$ m. We can again observe that the optimal position S

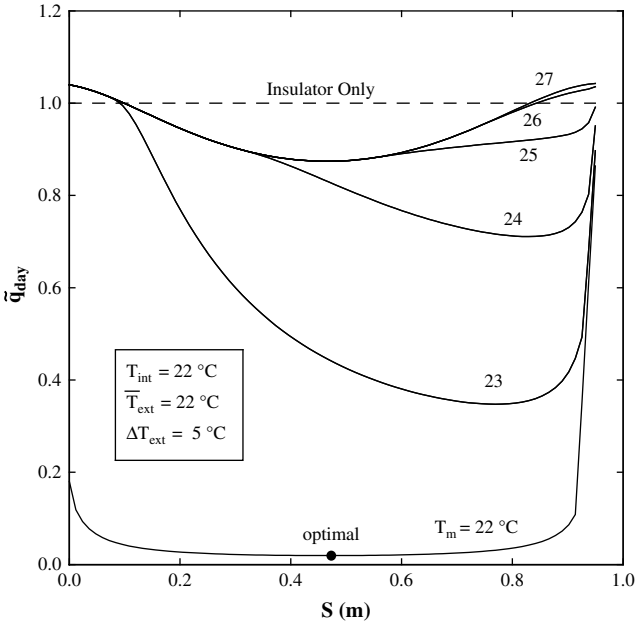

Fig. 5. Relative heat flow as a function of the PCM slab position and melting temperature when $\overline{T}_{ext} = T_{int}$.

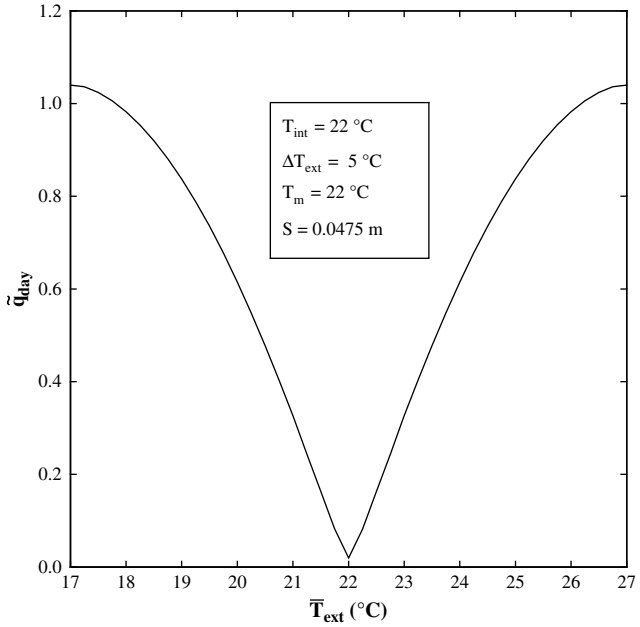

Fig. 6. Robustness of optimized wall with $\overline{T}_{ext} = T_{int}$ when $\overline{T}_{ext}$ changes.

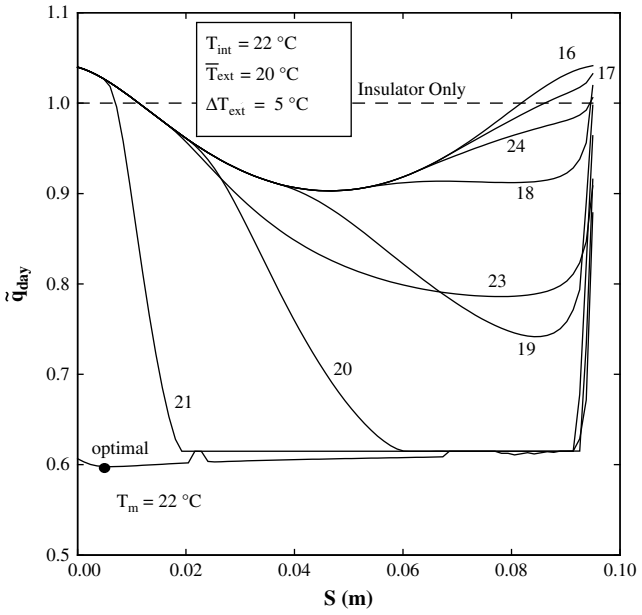

Fig. 7. Relative heat flow as a function of the PCM slab position and melting temperature when T_{int} is in the range (yet different) of $\overline{T}_{ext}$.

increases (i.e., moves toward the exterior side of the wall) as T_m differs from T_{int}, as expected from the qualitative analysis. For large (or small) T_m-values, our simulations yielded optimal positions S at the center of the wall because the thermal phase lag (due to heat capacity) dominates the thermal shielding (due to phase change). The robustness of this design with respect to the outdoor conditions ($\overline{T}_{ext}$) was also studied. We varied $\overline{T}_{ext}$ and calculated $\tilde{q}_{day}$ in each case. The results in Fig. 8 are similar to those of Fig. 6, i.e., as the outdoor temperature differs from the indoor temperature (22 °C), the shielding performance of the designed wall decreases up to the point when the designed wall performance is worst than a wall made of insulator only.

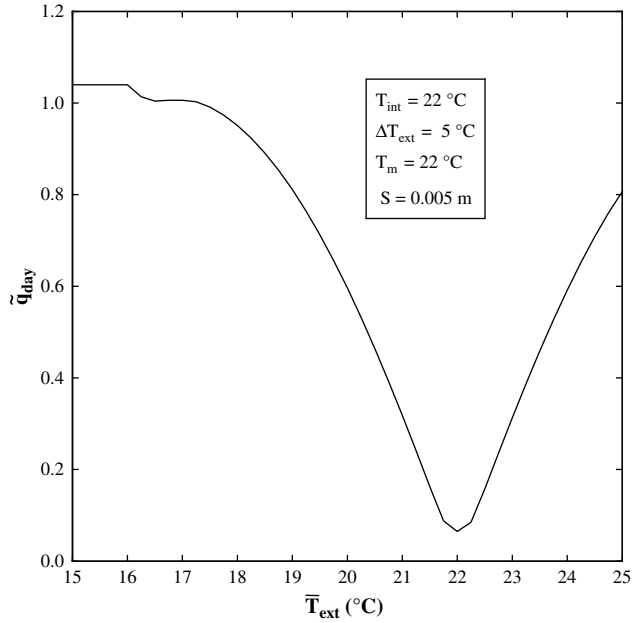

Fig. 8. Robustness of optimized wall with $\overline{T}_{ext} \neq T_{int}$ when $\overline{T}_{ext}$ changes.

4.2.3. Case III: T_{int} not within the range of T_{ext}(t)

The last case to consider is when the outdoor temperature is not within the range of T_{int}. For this purpose, we considered an exterior average air temperature of −2 °C. This case is akin to that shown in Fig. 3b. No gain compared to the reference wall was noted, no matter the position S or the melting temperature T_m. To explain why that is, we show in Fig. 9 the heat flux at $x = 0$ versus time with a wall made of insulator only (dashed line) and compare with a PCM layer ($T_m = 10$ °C) at three different positions (solid lines). Only the case with position $S = 0.0475$ m involves melting/solidification of the PCM during a cycle. Note that the integral (q_{day}) under the three solid curves is equal or greater than with the wall made of insulator only ($q_{day,ref}$). It has been verified that this holds true for any melting temperature and position in the wall. This corroborates with our qualitative argument in the end of Section 4.1, i.e., there is no shielding opportunities when T_{int} is not within the rage of T_{ext}. Moreover, the high conductivity of the PCM layer diminishes the total thermal resistance of the wall, which leads to $\tilde{q}_{day}$ value around 105%.

The important conclusions of the three cases considered in this section are that when the indoor air temperature is within the range of outdoor air temperature (cases I and II), considerable energy savings are possible (near 100% in ideal cases). However, when indoor air temperature is not within the range of outdoor air temperature (case III), small energy losses are to be expected compared to the completely insulator wall (∼5% for a wall in which the PCM occupies 5%). Note that these conclusions concern the shielding performance of the wall, and that PCMs may nevertheless be useful in building structure thanks to their large thermal inertia (damping of indoor air temperature). Since most walls perform in weather conditions in which both cases (cases II and III) are likely to occur throughout a whole year, an important question to answer is whether PCMs are beneficial for a yearly analysis. We will address that point in the subsequent sections.

5. Optimization procedure (genetic algorithms)

A genetic algorithm (GA) has been used to minimize the function q by varying the material composition of the wall. GAs are

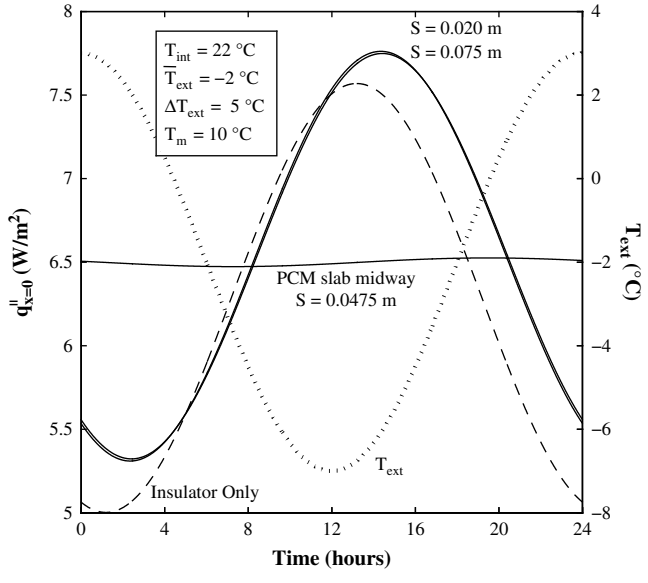

Fig. 9. Effect of the PCM slab on the indoor heat flux when outside temperature is far from inside temperature.

optimization tools relying on Darwinian evolution principles, and have been used successfully for the design of several heat transfer and energy systems. In particular, they have been able to determine optimal materials in many systems, e.g., [18–21]. We will not explain here the details of this algorithm that is becoming more and more common in the domain. Information is available elsewhere [22,23]. Only the main settings of our GA will be listed here.

The GA will vary the constitution of the wall in order to minimize q (Eq. (5)). In other words, the GA will determine the optimal material of each layer. Therefore, wall with several layers of PCMs will be possible. Each population is made of 30 individuals. Each individual (design) is coded with a binary representation. 3 bits are required to represent the material of each wall layer ($2^3 = 8$ different materials). Crossovers with two points are used, and the mutation rate was 3%. An elitist strategy was used, in such a way that the best 5 individuals from a population are ensured to propagate to the next generation. Convergence was declared when the best design was the same for 60 successive generations. Due to its probabilistic nature, two GA optimization runs with the same settings can yield different results. Therefore, we ran the GA 4 times for each problem to verify repeatability. These GA setting will be used in Sections 6 and 9.

6. Wall optimization based on idealized seasonal weather scenarios

In order to assess the annual behavior of a wall with PCM, we first considered a simplified model in which a typical daily periodic regime is sought during each of the four seasons. In other words, we found the periodic regime and calculated q_{day} for the average outdoor temperature of each season. Then, the total absolute heat transfer was achieved by adding the four absolute heat transfer of each season and multiplying by 91 days. This work was done for two locations: Québec City (QC, Canada) and Orlando (FL, USA), with summer, fall, winter, and spring average outdoor temperatures of 15, −2, −10, 10 °C and 27, 20, 17, and 25 °C respectively.

The wall of Fig. 1 has been decomposed into 20 layers, each layer having a thickness of 0.5 cm. The materials that are available to fill these layers are listed in Table 1, that is, one insulator, concrete and PCMs with different melting temperatures. Again, note that the GA may generate thick PCM slabs by placing several adjacent PCM layers in the wall. Considering 6 melting temperatures (i.e., $T_{\text{m}} = 20$, 21, 22, 23, 24, and 25 °C for Orlando, and 0, 4, 8, 12, 16, 20 °C for Québec City), the total number of possible materials is 8 for each layer. There are thus 2^{60} possible wall configurations. Four GA optimizations have been launched, each with different initial populations. The objective was to minimize the annual absolute heat transfer by varying the composition of the wall. The resulting designs for the weather data of Orlando are shown in Table 2. Each line of the table is the result of a full optimization. Layer 1 is the one closer to the interior. The GA found nearly equivalent optimal designs with only one layer of PCM and q as low as 32.1169 MJ/m^2, while the wall with insulator only yielded $q = 35.0948$ MJ/m^2 (more than 8% of reduction with the PCM). Note that the optimal designs identified by the GA did not selected concrete. The number of generations required to converge varied between 82 and 158, which means that less than 4000 of the possible designs have been simulated. Finally, these results match with conclusions from Section 4.1, i.e., it was expected that PCM may increase the performance of the wall for Orlando weather because the indoor temperature is within the range of outdoor temperature for the four seasons.

For the climate of Québec City, the GA never placed a PCM in the wall, i.e., the optimal design found by the GA was a wall made of insulator only, with $q = 149.77$ MJ/m^2. Again, these results corroborate with conclusions from Section 4.1, i.e., it was expected that PCM cannot increase the performance of the wall for Québec City weather because the indoor temperature is not within the range of outdoor temperature for most of the four seasons.

We will show in the next section, that PCM can actually benefit the wall performance even in cold climate. However, a more refined model is required to capture that benefit.

7. Wall optimization based on real weather data including radiation

The following sections present a test case to apply the results and methods developed in the previous sections. The idea of introducing PCM layers within the wall in order to enhance its overall thermal inertia has been validated with simulations involving real weather data for Québec City. The data used in the simulations are those of 1997 and 1998. In fact, the year 1997 is used solely in order to estimate the temperature profile within the wall at the beginning of 1998, and the resulting heat flows q_{year} presented here are those of 1998. The outdoor air temperature and total solar irradiation on a horizontal surface were recorded by Environment Canada every hour at the Jean-Lesage airport in Québec City. In order to be more realistic we included solar heat gain at the outer surface of the wall. Therefore the boundary condition at $x = L$ for this part of the paper becomes

$$k\left.\frac{\partial T}{\partial x}\right|_{x=L} = h_{\text{ext}}(T_{\text{ext}} - T(x = L)) + \alpha G_{\text{sun}} \tag{9}$$

where α is the solar absorptivity of the surface and G_{sun} is the solar irradiation on the wall. For simplicity, the α-value used here is 1. Since the wall is vertical, the experimental total irradiation (diffuse and direct) was translated from horizontal irradiation into

Table 2
Wall designs achieved by the GA with idealized annual simulation for Orlando (FL, USA).

Run	N_{gen}	Optimized material in each layer																			q_{year}(MJ/m^2)
		1	2	3	4	5	6	7	8	9	10	11	12	13	14	15	16	17	18	19	20	
#1	158	[a]													22[b]							32.117202
#2	105						22															32.117119
#3	82																			22		32.117347
#4	149								22													32.116912

[a]Blue: insulator layer.
[b]Red: PCM layer (with specified T_{m}). For interpretation of color in Table 2, the reader is referred to the web version of this article.

irradiation on a vertical surface (oriented southward), with the appropriate relations for solar radiation geometry [15].

For annual analysis, mesh and time-step independences were tested extensively. Mesh was refined by successive doubling up to the point when the heat flow q_{year} (satisfying time-step independence) varied by less than 0.5%. The time-step independence for each mesh is satisfied when the heat flow q_{year} varies by less than 0.1% for consecutive time-step divisions by 2. The results showed that for an annual investigation with weather data, 130 control volumes with a time step of 3600 s (1 h) were sufficient to provide that precision. This numerical setup will be used in Sections 8 and 9.

8. Parametric study with weather data (outside temperature and solar radiation)

Even before performing the complete wall optimization, we studied the effect of a single PCM layer within the wall as in Section 4 but this time with the real set of annual weather data described above (see Fig. 4 for wall description). This will allow to quantify the impact of real boundary conditions on the objective function and help understanding the results of the full optimization (Section 9). The melting temperature and position of the PCM layer have been varied. The results ($\tilde{q}_{year}$ defined similarly to Eq. (8)) are presented in Fig. 10. It is observed that a melting temperature of 22 °C and a PCM positioned slightly closer to the interior façade ($S = 0.025$ m) constitute the optimal wall design. This design yields $q_{year} = 110.1594$ MJ/m^2 and $\tilde{q}_{year} = 0.931$. Fig. 10 agrees well with conclusions (i)–(iv) of Section 4.1, because the PCM is active during the summer, i.e., when outdoor temperature is closer to the indoor temperature. But during winter, the PCM is inactive (and even detrimental due to its high thermal conductivity). The net gain during the summer is sufficient to counterbalance the losses of thermal resistance in the winter due to a layer of insulator replaced by a PCM. Over the year, with the optimal PCM slab position and melting temperature, a reduction of 7% of the absolute heat transfer is noted compared to a wall made of insulator only. This effect was not observed with the idealized and simplified model of Section 5. It is found that the detailed transient outdoor temperature and solar radiation are required in order to determine the potential of PCMs in building envelopes in cold climates.

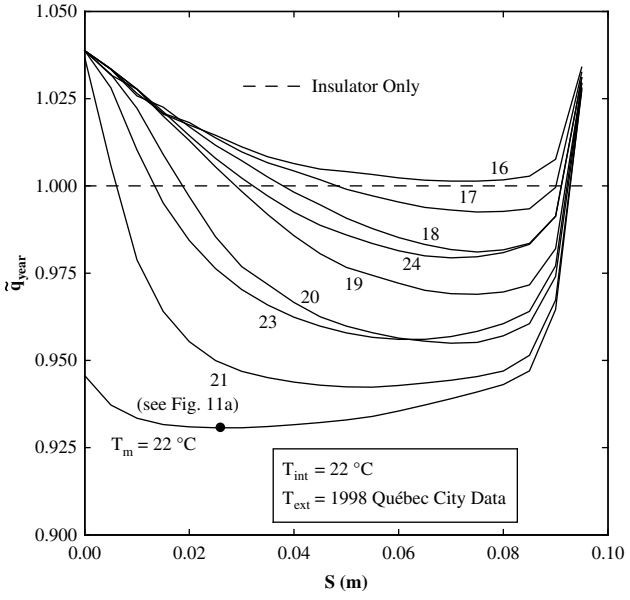

Fig. 10. Relative heat flow as a function of the PCM slab position and melting temperature using Québec City weather data (1997–1998).

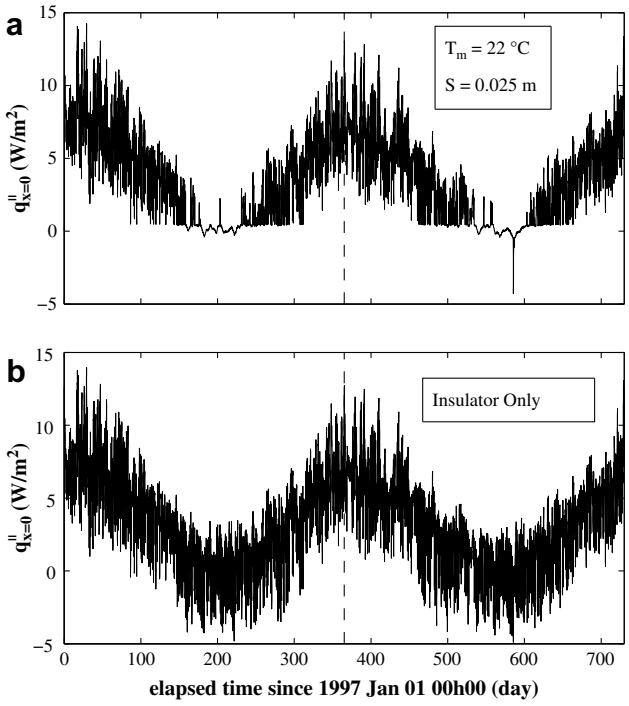

Fig. 11. Indoor heat flux using Québec City weather data (1997–1998) with (a) the optimized wall from Fig. 10, (b) the wall made of insulator only.

Finally, the indoor heat flux with optimal PCM position and melting temperature is plotted in Fig. 11a as a function of time. For the sake of comparison, the indoor heat flux for the reference wall (insulator only) is shown in Fig. 11b. Recall that only the 1998 heat flow information in Fig. 11 (right-hand side of the vertical dashed line) is used to calculate q_{year}. 1997 data are used only to estimate the temperature profile in the wall at the beginning of 1998. The PCM clearly has the effect of shielding the heat gains during the summer and has a relatively weak impact in the winter. Observe in Fig. 11a that the shielding effect is briefly broken (just before the day 600). This is because the PCM has completely melted and thus becomes useless until it re-solidifies. Finally, it is instructive to observe that the optimal PCM melting temperature, even in a yearly analysis, stays nearly equal to the indoor temperature.

9. Genetic algorithm optimization based on real weather data

Finally, the GA was used to fully optimize the wall inner structure when the weather data for Québec City (1997–1998) are used. The wall configuration is the same as in Section 6, i.e., the wall is 10 cm-thick and is divided in 20 layers of 0.5 cm. Eight kinds of materials are used for the optimization; an insulator, concrete, and 6 PCMs with different melting temperatures ($T_m = 20, 21, 22, 23, 24$ and 25 °C). Again, the GA has the freedom to generate thick PCM slabs by placing several adjacent PCM layers in the wall. These temperatures were chosen relying on the results of the preceding sections; it is expected that PCMs are useful when they are active during summer. Four runs of the GA were performed. The number of generations for convergence was similar to that obtained previously. The results of the GA optimization are shown in Table 3. Note that concrete was never selected in optimized walls. The GA found optimal designs with one layer of PCM giving q_{year} as low as 110.1594 MJ/m^2, compared to a wall made of insulator that yields

Table 3
Wall designs achieved by the GA with real weather data (temperature and solar irradiation) in Québec City (QC, Canada).

Run	N_{gen}	Optimized material in each layer																				q_{year} (MJ/m^2)
		1	2	3	4	5	6	7	8	9	10	11	12	13	14	15	16	17	18	19	20	
#1	117	[a]					22[b]															110.1594
#2	136															22						111.14568
#3	123								22													110.19928
#4	138									22												110.26099

[a]Blue: insulator layer.
[b]Red: PCM layer (with specified T_m). For interpretation of color in Table 3, the reader is referred to the web version of this article.

$q_{year,ref} = 118.3626$ MJ/m^2 (7% of reduction with the PCM). The melting temperature of the slab is 22 °C with the four optimizations, and the optimal position is in the vicinity of the center of the wall. It is also interesting to note that the GA positioned only one PCM layer in the wall. Too many PCM layers would decrease the total thermal resistance of the wall (due to the high thermal conductivity of PCM). Hence, these optimal designs are the results of a tradeoff between the shielding effect of PCMs and the insulation effect of the polystyrene. From a construction and cost point-of-view, it is useful to know that a single PCM layer is actually the optimal configuration.

Even though the 4 runs of the GA generated slightly different optimal walls, they all have a similar performance, which corroborates the robustness in regard of the PCM position observed in Fig. 10.

Finally, note that these optimal designs differ from those obtained in Section 6, in which the GA yielded wall with insulator only (no PCM) for Québec City. The boundary conditions were too simple in Section 6 (annual temperature was modeled with 4 idealized seasons and solar irradiation was not considered) and were not adequate to capture the advantage of PCM slabs in the wall for cold climate as in Québec City. The annual absolute heat flow was 149.77 MJ/m^2 in Section 6 with the idealized weather data. With the more accurate boundary conditions used in this section, the annual absolute heat flow is smaller either for the reference wall (118.3626 MJ / m^2). The error associated with the idealized boundary conditions is thus of the order of 25%, i.e., much larger than the benefit envisioned here ($\sim$7%).

10. Conclusions

The thermal shielding performance of an idealized wall containing PCM layers is numerically modeled, analyzed, and maximized in this paper. The wall model is simple enough to provide fundamental results that may help to understand the impact of PCM when it is integrated in real building envelope or in other systems. Simulations with recorded weather data were also performed. The main conclusions of this study could be formulated as follows:

- A parametric study has been performed for a 10 cm wall with a single 0.5 cm PCM slab for different harmonic boundary conditions representing outdoor conditions. It revealed that the melting temperature and position of the PCM slab have a large influence on the shielding performance of the wall when the indoor temperature (22 °C) is in the range of the outdoor temperature. Melting temperatures close to 22 °C and slabs close to the center led to the best performances. When the indoor temperature is far from the range of the outdoor temperature, the PCM slab is detrimental to the wall performance. Therefore, in cold climates, the shielding effect of PCM is likely to be active in the summer but not in the winter.
- Full optimizations of the wall composition with genetic algorithm (GA) were performed. The GA had a possibility to combine different materials and PCM melting temperatures in the wall. The wall composition based on a simplified yearly analysis with idealized harmonic outdoor temperature did not produce designs with PCMs for Québec City, but included PCMs for Orlando. However, a yearly optimization based on real weather data (including solar radiation impinging the wall) generated wall designs with a single PCM slab, even for Québec City data (optimal melting temperature of 22 °C and optimal position close to the wall centerline).
- Genetic algorithms are a useful tool to identify rapidly the best material composition (including PCMs) of a wall. Only a small fraction of all possible designs needs to be tested.

In the future, it would be interesting to perform a thermoeconomic analysis of walls with PCMs. The idea would be to vary the wall composition and also its thickness in order to minimize the total annualized cost (summation of the cost of the wall and cost of heating/cooling). A GA could be used to perform that work, and would yield in that case not only the wall composition, but also its optimal thickness and minimized price. More materials' possibilities (including other types of PCMs) could also be included in the database. It is important to keep in mind that the boundary conditions applied on the wall surfaces have shown to have a great impact on the results (idealized versus real outdoor temperature and solar radiation). Furthermore, internal building components (walls, floors) could also benefit from the use of PCMs to increase the building thermal inertia. Other objective functions, including entropy generation [24] could also be investigated.

Acknowledgement

The authors' work was supported by the Natural Sciences and Engineering Research Council of Canada (NSERC).

References

[1] O. Kaynakli, A study on residential heating energy requirement and optimum insulation thickness, Renewable Energy 33 (6) (2008) 1164–1172.
[2] H. Asan, Effects of wall's insulation thickness and position on time lag and decrement, Energy and Buildings 28 (3) (1998) 299–305.
[3] H. Asan, Numerical computation of time lags and decrement factors for different building materials, Building and Environment 41 (5) (2006) 615–620.
[4] M. Ciampi, F. Fantozzi, F. Leccese, G. Tuoni, On the optimization of building envelope thermal performance – multi-layered wall design to minimize heating and cooling plant intervention in the case of time varying external

temperature fields, Civil Engineering and Environmental Systems 20 (4) (2003) 231–254.
[5] Y. Zhang, G. Zhou, K. Lin, O.H. Zhang, H. Di, Application of latent heat thermal energy storage in buildings: state-of-the-art and outlook, Building and Environment 42 (6) (2007) 2197–2209.
[6] Z.-X. Gong, A.S. Mujumdar, Enhancement of energy charge-discharge rates in composite slabs of different phase change materials, International Journal of Heat and Mass Transfer 39 (4) (1996) 725–733.
[7] E.M. Alawadhi, Thermal analysis of a building brick containing phase change material, Energy and Buildings 40 (3) (2008) 351–357.
[8] K.A.R. Ismail, J.N.C. Castro, PCM thermal insulation in buildings, International Journal of Energy Research 21 (14) (1997) 1281–1296.
[9] J.-S. Kim, K. Darkwa, Simulation of an integrated PCM-wallboard system, International Journal of Energy Research 27 (3) (2003) 215–223.
[10] F. Kuznik, J. Virgone, J.-J. Roux, Energetic efficiency of room wall containing PCM wallboard: a full-scale experimental investigation, Energy and Buildings 40 (2) (2008) 148–156.
[11] E.F. Helmut, C. Stetiu, Thermal performance of phase change wallboard for residential cooling application, Report of Energy and Environment Division, University of California, USA, 1997, p. 24.
[12] D. Heim, J.A. Clarke, Numerical modeling and thermal simulation of PCM–gypsum composites with ESP-r, Energy and Buildings 36 (8) (2004) 795–805.
[13] Canadian climate normals or averages 1971–2000, Environment Canada, http://www.climate.weatheroffice.ec.gc.ca.
[14] Typical high and low temperature for various Florida cities, US Travel Weather (2008).www.ustravelweather.com.
[15] F.C. McQuiston, J.D. Parker, Heating, Ventilating, and Air Conditioning, sixth ed. Wiley, 2005.
[16] M.M. Farid, A.M. Khudhair, S.A.K. Razack, S. Al-Hallaj, A review on phase change energy storage: materials and applications, Energy Conversion and Management 45 (9–10) (2004) 1597–1615.
[17] H. Hu, S.A. Argyropoulos, Mathematical modelling of solidification and melting: a review, Modelling and Simulation in Materials Science and Engineering 4 (4) (1996) 371–396.
[18] M. Tye-Gingras, L. Gosselin, Thermal resistance minimization of a fin-and-porous medium heat sink with evolutionary algorithms, Numerical Heat Transfer – Part A: Applications 54 (4) (2008) 349–366.
[19] C. Villemure, L. Gosselin, G. Gendron, Minimizing hot spot temperature of porous stacking in natural convection, International Journal of Heat and Mass Transfer 51 (15–16) (2008) 4025–4037.
[20] G. Leblond, L. Gosselin, Effect of non-local equilibrium on minimal thermal resistance porous layered system, International Journal of Heat and Fluid Flow 29 (1) (2008) 281–291.
[21] P. Wildi-Tremblay, L. Gosselin, Layered porous media architecture for maximal cooling, International Journal of Heat and Mass Transfer 50 (3–4) (2007) 464–478.
[22] M. Mitchell, An Introduction to Genetic Algorithms, MIT Press, 1998.
[23] L. Gosselin, M. Tye-Gingras, F. Mathieu-Potvin, Review of the utilization of genetic algorithms in heat transfer problems, International Journal of Heat and Mass Transfer 52 (9–10) (2009) 2169–2188.
[24] F. Strub, J. Castaing-Lasvignottes, M. Strub, M. Pons, F. Monchoux, Second law analysis of periodic heat conduction through a wall, International Journal of Thermal Sciences 44 (12) (2005) 1154–1160.